Bioorganic & Medicinal Chemistry 25 (2017) 3980–3988

Contents lists available at ScienceDirect

Bioorganic & Medicinal Chemistry

journal homepage: www.elsevier.com/locate/bmc

Synthesis, docking study and neuroprotective effects of some novel pyrano[3,2-*c*]chromene derivatives bearing morpholine/phenylpiperazine moiety

Bilqees Sameem [a], Mina Saeedi [b,c], Mohammad Mahdavi [d], Hamid Nadri [e], Farshad Homayouni Moghadam [f], Najmeh Edraki [g], Muhammad Imran Khan [h], Mohsen Amini [i,d,*]

[a] *Faculty of Pharmacy, International Campus (TUMS-IC), Tehran University of Medical Sciences, Tehran, Iran*
[b] *Medicinal Plants Research Center, Faculty of Pharmacy, Tehran University of Medical Sciences, Tehran, Iran*
[c] *Persian Medicine and Pharmacy Research Center, Tehran University of Medical Sciences, Tehran, Iran*
[d] *Drug Design & Development Research Center, Tehran University of Medical Sciences, Tehran, Iran*
[e] *Department of Medicinal Chemistry, Faculty of Pharmacy, Shahid Sadoughi University of Medical Sciences, Yazd, Iran*
[f] *Department of Cellular Biotechnology at Cell Science Research Center, Royan Institute for Biotechnology, ACECR, Isfahan, Iran*
[g] *Medicinal and Natural Products Chemistry Research Center, Shiraz University of Medical Sciences, Shiraz, Iran*
[h] *Department of Pharmacology, School of Medicine TUMS-IC, Tehran, Iran*
[i] *Department of Medicinal Chemistry, Faculty of Pharmacy and Drug Design & Development Research Center, Tehran University of Medical Sciences, Tehran, Iran*

ARTICLE INFO

Article history:
Received 9 February 2017
Revised 4 May 2017
Accepted 18 May 2017
Available online 19 May 2017

This manuscript is dedicated to the fond memory of Professor Abbas Shafiee.

Keywords:
Alzheimer's disease
Cholinesterase inhibition
Coumarins
Neuroprotection
β-Secretase inhibition

ABSTRACT

Novel pyrano[3,2-*c*]chromene derivatives bearing morpholine/phenylpiperazine moiety were synthesized and evaluated against acetylcholinestrase (AChE) and butylcholinestrase (BuChE). Among the synthesized compounds, *N*-(3-cyano-4-(4-methoxyphenyl)-5-oxo-4,5-dihydropyrano[3,2-*c*]chromen-2-yl)-2-(4-phenylpiperazin-1-yl)acetamide (**6c**) exhibited the highest acetylcholinestrase inhibitory (AChEI) activity (IC_{50} = 1.12 μM) and most of them showed moderate butylcholinestrase inhibitory activity (BChEI). Kinetic study of compound **6c** confirmed mixed type of inhibition towards AChE which was in covenant with the results obtained from docking study. Also, it was evaluated against β-secretase which demonstrated low activity (inhibition percentage: 18%). It should be noted that compounds **6c**, **7b**, **6g**, and **7d** showed significant neuroprotective effects against H_2O_2-induced PC12 oxidative stress.

1. Introduction

Alzheimer's disease (AD) is a multifactorial, progressive neurodegenerative disorder of the central nervous system (CNS) associated with cognitive impairment and decline in language ability among elderly people.[1] Many factors are believed to play role in the disease onset and progression. Studies have revealed that the decrease in acetylcholine neurotransmitter,[2] β-amyloid aggregation due to the cleavage of amyloid precursor protein (APP),[3] irregular phosphorylation of tau proteins, and subsequently formation of neurofibrils tangles in the hippocampal neurons leading to cell death.[4] Furthermore, other parameters such as inflammation conditions and oxidative stress play a critical role in the pathogenesis of AD.[5] In addition to the hydrolytic role of AChE, it induces pro-aggregation of amyloids and deposition into the neurofibrils (non-catalytic role).[6] Accordingly, the inhibition of this enzyme is considered as a main approach increasing the cholinergic transmission, prevention of amyloid aggregation and hence a vital strategy to palliate the disease symptoms.[7] In normal healthy brain, AChE plays predominant role and butylcholinesterase (BuChE) a minor role in the hydrolysis of ACh. As AD progresses, the level of AChE decreases or remains unchanged whereas BuChE increases in certain regions of brain probably to offset the deficiency of AChE.[8] Selective or non-selective inhibition of BuChE represents legitimate therapeutic role in alleviating the disease symptoms as its inhibition has shown some significant results in recent years.[9] Also, compounds with additional pharmacological effects such as neuroprotective, anti-oxidative, and β-secretase inhibitory

* Corresponding author at: Department of Medicinal Chemistry, Faculty of Pharmacy and Drug Design & Development Research Center, Tehran University of Medical Sciences, Tehran, Iran.
E-mail address: moamini@sina.tums.ac.ir (M. Amini).

http://dx.doi.org/10.1016/j.bmc.2017.05.043
0968-0896/

activity can be considered as a benefit way in AD symptomatic treatment.[10,11]

Pertinently, Donepezil, Rivastigmine, Tacrine, Galantamine (Fig. 1), the four among five FDA approved drugs, are acetylcholinestrase inhibitors and are used for the symptomatic treatment of AD in the early and mild stages.[12,13]

Coumarins are naturally occurring phytochemicals; studies have shown that both naturally and synthetic coumarin-based scaffolds (Fig. 2) exhibit potent AChE inhibitory activity with some additional important pharmacological features. Previous studies have demonstrated that coumarin moiety primarily interacts with the peripheral anionic site (PAS) of AChE and when linked by an appropriate spacer such as benzyl amine, phenylpiperazine, or aniline moieties, interacts with catalytic anionic site (CAS).[14]

Dual binding coumarin-based compounds such as AP 2238[15] and Ensaculin (coumarin-based derivative containing a phenylpiperazine moiety) are under clinical investigations (Fig. 2).[16] Therefore, dual binding site coumarin-based scaffolds with some other pronounced pharmacological effects are of vital interest in the therapeutics of the disorder. Herein, in continuation of our work on the synthesis of anti-cholinesterase (anti-ChE) and neuroprotective agents,[17–22,25] we report synthesis and anti-ChE activity of some novel pyrano[3,2-*c*]chromenes bearing morpholine/phenylpiperazine moiety **6** and **7** (Fig. 2).

2. Results and discussion

2.1. Chemistry

The synthetic route for the synthesis of target compounds **6** and **7** is shown in Scheme 1.

The required starting materials **4** were prepared in high yields (85–95%) through one-pot multicomponent reaction of 4-hydroxycoumarin (**1**), malanonitrile (**2**), and different aromatic aldehydes **3** in the presence of DABCO in ethanol at room temperature. In the next step, reaction of chloroacetylchloride and compound **4** in DMF at ambient temperature for 24 h led to the formation of the corresponding amide **5**. It should be noted that the later reaction was initiated at 0 °C to avoid vigorous reaction and the reaction was left to stir at room temperature. Then, compound **5** was treated with phenylpiperazine/morpholine to undergo nucleophilic substitution reaction in the presence of KI in methanol under reflux conditions for 18–20 h. The Structures of all target compounds were elucidated by IR and NMR spectroscopy as well as mass spectrometry.

2.2. Anti-AChE and anti-BuChE activities

The target compounds **6** and **7** containing phenylpiperazine and morpholine moiety, respectively were evaluated for their AChE and BuChE inhibitory activity *in vitro* according to Ellman's modified method[23] using marketed drug donepezil as standard (Table 1). Compounds in series **6** usually showed better anti-AChE activity comparing series **7**. In this category, compound **6c** having strong electron donating group (OMe) at 4- position demonstrated the most potent activity (IC_{50} = 1.12 μM). An additional methoxy group at 3- position led to slight decrease of anti-AChE activity in compound **6e** (IC_{50} = 1.42 μM). Insertion of an additional electron donating OCH_3-group at position 3 in compound **6e** led to onefold decline in inhibitory activity apparently due to the steric hindrance. Similar SAR trend was observed in a study demonstrating that the introduction of an additional OCH_3 group on the tetrahydrochromeno pyrano [2,3-*b*]quinoline scaffold led to 2.6-fold decline in activity (IC_{50} = 43 nM), while insertion of a third OCH_3 group showed nearly 5- fold decline in activity (IC_{50} = 69 nM).[22] However, the introduction of methoxy group at position 4 in compound **6d** resulted in 28-fold decrease in activity which is in analogy with the docking studies as depicted in Fig. 5.

It was convinced that the position of methoxy groups played an important role in AChEI since compound **6d** possessing two methoxy groups at 2- and 4-positions of pendant aryl group showed significant decrease in anti-AChE activity (IC_{50} = 31.4 μM). It is concluded that the enzyme has good tolerance at position 3 for an extra methoxy group and not at position 2.

Our results showed that insertion of moderate electron donating group (Me) into 2- and 4- positions of aryl group (**6b**) exhibited nearly equal anti-AChE activity (IC_{50} = 32.9 μM) as that of compound **6d**. However, presence of 4-Cl (**6g**) on the aryl group led to relatively good activity (IC_{50} = 6.33 μM). Compound **6a** with no substituents on aryl group showed moderate inhibitory activity (IC_{50} = 11.5 μM). It should be noted that the inhibitory activity of compounds **6f** and **6h** could not be evaluated because the compounds were insoluble in buffer solution.

Compounds in series **6** were evaluated for their anti-BuChE activity. Totally, they showed insignificant inhibitory activity and compound **6c** was the most active BuChE inhibitor with IC_{50} = 45.7 μM.

From Table 1, compounds in series **7** showed moderate to good AChEI activity. Compound **7b** possessing strong electron donating group (OMe) at 4- position showed highest inhibitory activity with IC_{50} = 2.05 μM. Similar to series **6**, introduction of two methoxy groups into positions 3- and 4- of aryl group **7d** led to the decrease of anti-AChE activity as IC_{50} was obtained 3.25 μM. Also, insertion of methoxy group to positions 2- and 4- afforded much lower AChEI activity (**7c**, IC_{50} = 25.6 μM). Here again, the similar reason could be justified for antithetical activity of compounds **7c** and **7d** that mentioned for **6c** and **6d**.

Pertinent to mention, the presence of electron withdrawing group (NO_2, **7g**) as well as heterocyclic ring (thiophene, **7h**) led to the loss of inhibitory activity (IC_{50} >100 μM). Unsubstituted phenyl ring **7a** showed moderate anti-AChE activity (IC_{50} = 23.9 μM). Another point is related to halogenated aryl groups which showed different activities toward AChE. 4-F substituted derivative **7e** did not show activity, whereas 4-Cl substituted derivative **7f** exhibited relatively good AChEI activity (IC_{50} = 14.6 μM). BuChE inhibitory activity of compounds in series **7** except **7d** (IC_{50} = 34.2 μM) indicated low inhibitory activity.

Overall, our results confirmed that 4-OMe phenyl group played an imperative role in anti-AChE activity since **6c** and its analogue **7b** possessing phenylpiperazine and morpholine, respectively

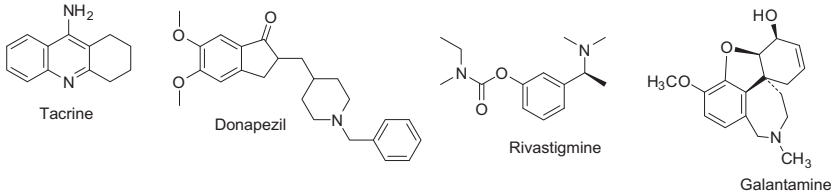

Fig. 1. Structures of approved AChE inhibitors.

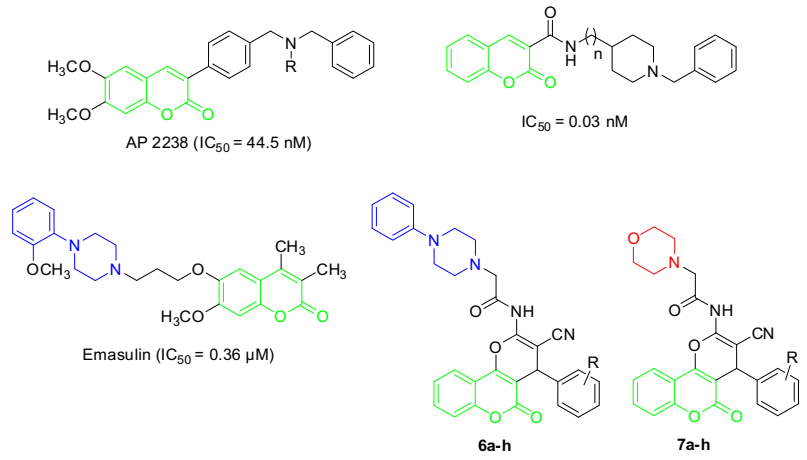

Fig. 2. Structures of some coumarin-based scaffolds and designed compounds (**6a–h** and **7a–h**).

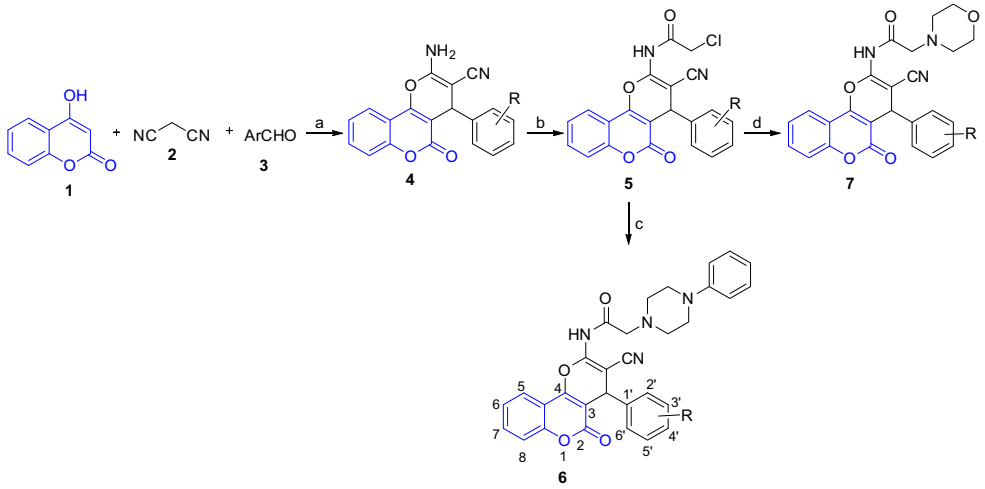

Scheme 1. Synthesis of desired compounds **6a–h** and **7a–h**, Reagents and conditions: (a) DABCO, EtOH, rt, 24 h; (b) Chloroacetyl chloride, DMF, rt, 24 h; (c) Phenylpiperazine, KI, MeOH, reflux 18–24 h; (d) morpholine, KI, MeOH, reflux 18–24 h.

showed the best activities. Also, similar results were observed for compounds having two methoxy groups (**6d**, **6e**, **7c**, and **7d**). Clearly, presence of two methoxy groups at 3- and 4- positions induced much higher activity (Table 1). Although presence of chlorine in two series **6g** and **7f** led to relatively good activity, compound **6g** exhibited higher inhibitory activity more than two fold confirming the significant role of phenylpiperazine. In the same manner, in the case of compounds possessing phenyl moieties **6a** and **7a**, presence of phenylpiperazine increased AChEI activity by two fold.

As mentioned above, no remarkable anti-BuChE activity was displayed by compounds **6** and **7**. Only, compound **7d** showed moderate anti-BuChE activity among the synthesized compounds **6** and **7**.

Finally, the best selectivity (BuChE/AChE) was related to compound **6e** by the selectivity index (SI) = 41.0. Also, the most potent anti-AChE compound **6c** showed almost similar SI by 40.8.

2.3. Kinetic study of AChE inhibition

The most active compound **6c** was subjected to kinetic studies to obtain the kinetic mode of AChE inhibition. For this purpose, the rate of enzyme activity was measured in the presence of four different concentrations of inhibitor (0.62, 1.23, and 2.47 μM) and different concentrations of acetylthiocholine as substrate (ATCh, [S]). For each inhibitor concentration, the initial velocity was measured at different substrate concentrations and the reciprocal of the initial velocity (1/v) was plotted *vs* the reciprocal of substrate concentration (1/[S]). As shown in Fig. 3, the obtained double reciprocal (Lineweaver-Burk) plot represents a mixed-type inhibition pattern for compound **6c**. The Ki value was also calculated using the secondary plot (Ki = 3.19 μM) (Fig. 3). All experiments were performed based on the Ellman's method as described for *in vitro* AChEI evaluation.

2.4. Neuroprotective activity against H_2O_2 induced apoptosis in PC12 neuron cells

The neuroprotective effects of compounds **6c**, **6e**, **6g**, **7b**, and **7d** against H_2O_2 induced oxidative stress and apoptosis in PC12 neuron cells were evaluated using Methylthiazol Tetrazolium (MTT) assay (Fig. 4). The differentiated cells were pretreated with different concentrations of compounds **6c**, **6e**, **6g**, **7b**, and **7d** at 10, 50, and100 μM. As shown in Fig. 4, the percent of cell viabilities were calculated in comparison to control group. Compounds **6c**, **6e**, **6g**, **7b**, and **7d** demonstrated good neuroprotectivity at different concentration and showed cell viability of 84.7, 76.0, 75.0, 78.5, and 84.7%, respectively at 10 μM with quercetin as internal standard.

Table 1
AChE and BuChE inhibitory activity of compounds **6a–h** and **7a–h**.

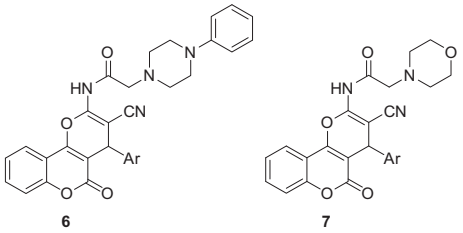

Entry	Products **6**/**7**	Ar	IC_{50} μM (AChE)[a]	IC_{50} μM (BuChE)[a]	SI[b]
1	**6a**	C_6H_5	11.5 ± 1.72	52.3 ± 4.18	4.5
2	**6b**	2,4-$DiCH_3C_6H_3$	32.9 ± 5.51	>100	–
3	**6c**	4-$OCH_3C_6H_4$	1.12 ± 0.43	45.7 ± 4.32	40.8
4	**6d**	2,4-$DiOCH_3C_6H_3$	31.4 ± 4.72	>100	–
5	**6e**	3,4-$DiOCH_3C_6H_3$	1.42 ± 0.23	58.2 ± 4.56	41.0
6	**6f**	4-FC_6H_4	n.d[c]	n.d[c]	–
7	**6g**	4-ClC_6H_4	6.33 ± 1.77	89.2 ± 6.97	14.1
8	**6h**	4-$NO_2C_6H_4$	n.d[c]	n.d[c]	–
9	**7a**	C_6H_5	23.9 ± 4.60	88.4 ± 6.28	3.7
10	**7b**	4-$OCH_3C_6H_4$	2.05 ± 0.58	63.8 ± 2.68	31.1
11	**7c**	2,4-$DiOCH_3C_6H_3$	25.6 ± 1.11	>100	–
12	**7d**	3,4-$DiOCH_3C_6H_3$	3.25 ± 0.55	34.2 ± 5.74	10.5
13	**7e**	4-FC_6H_4	>100	>100	–
14	**7f**	4-ClC_6H_4	14.6 ± 2.50	91.5 ± 8.18	6.3
15	**7g**	4-$NO_2C_6H_4$	>100	>100	–
16	**7h**	2-Thiophene	>100	>100	–
17	Donepezil		0.031 ± 0.007	8.73 ± 2.27	

[a] Inhibitor concentration (mean ± SD of three experiments) required for 50% inactivation of AChE.
[b] Selectivity index = IC50 (buChE)/IC50 (AChE).
[c] They were insoluble in buffer assay.

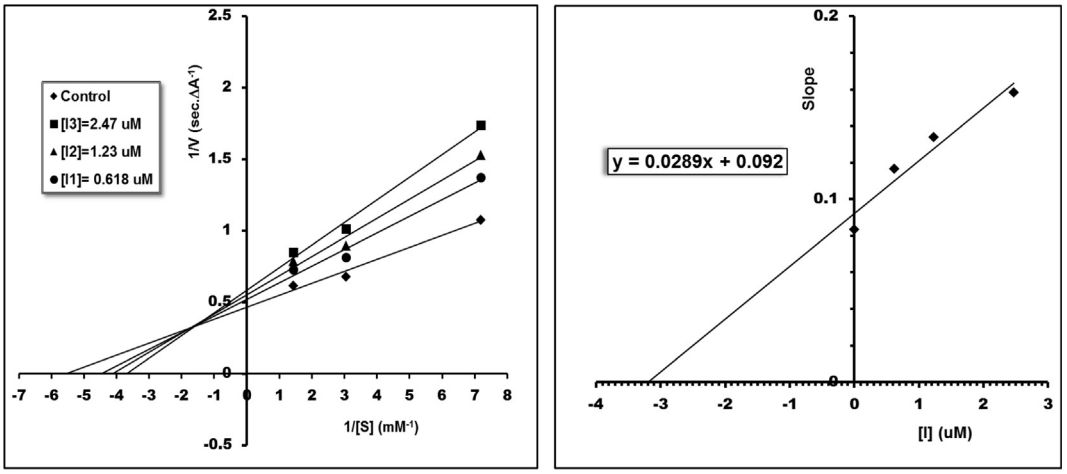

Fig. 3. *Left*: Lineweavere-Burk plot for the inhibition of AChE by compound **6b**; *Right:* Secondary plot for calculation of steady-state inhibition constant (Ki) of compound **6b.**

Statistical analysis of the data was performed using One-way ANNOVA ordinary method, significance of the results was determined by Tukey's test.

2.5. BACE-1 inhibitory activity of compound *6c*

The BACE-1 inhibitory activity of **6c** was evaluated by fluorescence resonance emission transfer (FRET) method. The kit consists of enzyme BACE-1 and APP peptide based substrate (Rh-EVNL-DAEFK-quencher) comparing with OM99-2 (IC_{50} = 0.014 μM) as the reference. Compound **6c** displayed demonstrated low activity (inhibition percentage: 18%).

2.6. Docking

To clarify the mode of interaction of the most potent compound **6c** in the active site of AChE, docking study was conducted using Auto dock Vina 1.1.2. For this purpose, the ligand-bonded crystallographic structure of AChE with PDB ID: 1eve was retrieved from RCSB protein data bank. The best docked pose of each ligand in

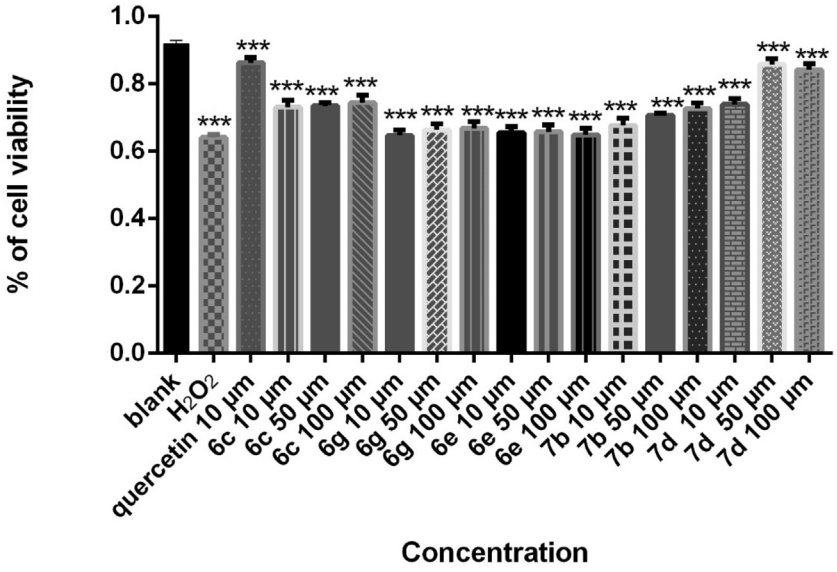

Fig. 4. Neuroprotective activity of compounds **6c**, **6e**, **6g**, **7b**, and **7d** on PC12 cells against H_2O_2 induced cells death. ($^{***}P < 0.001$) represents the significance with respect to blank.

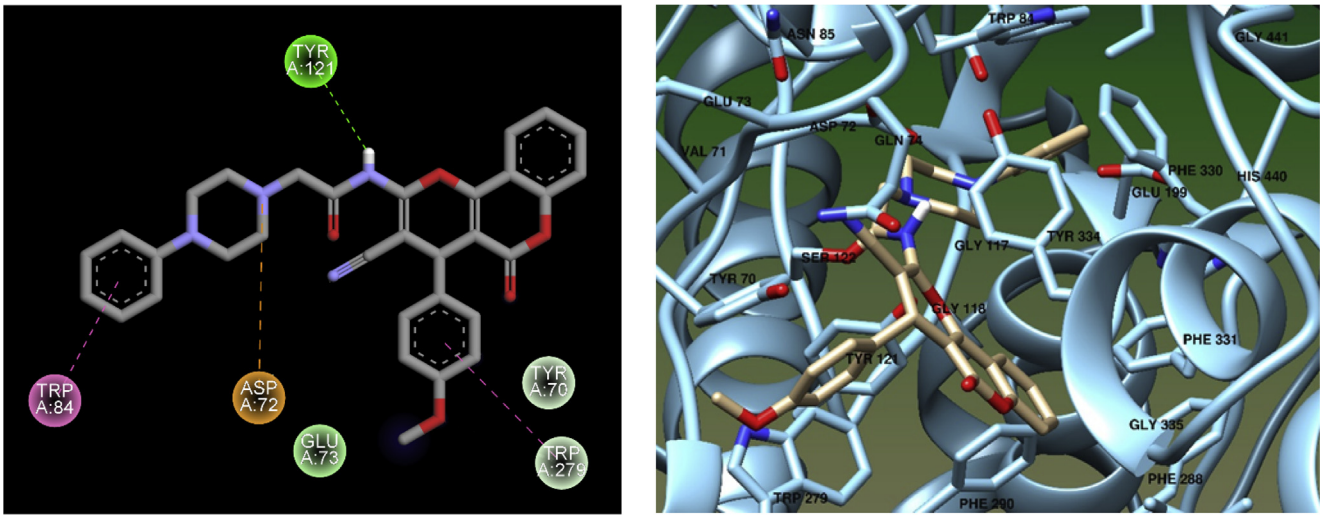

Fig. 5. *Left*: Two dimensional mode of interaction of compound **6c** with AChE. *Right*: Three dimensional mode of interaction of compound **6c** with AChE. Hydrogen bond and hydrophobic as well as ionic interactions are shown by green, pink, and yellow, respectively.

terms of the free energy of binding was extracted. The best docked pose of compound **6c** was subjected to further studies of binding mode. As depicted in Fig. 5, the phenylpiperazine moiety oriented towards the bottom of active site where the phenyl ring interacted with Trp84 (in the CAS) through a π-π stacking. In this orientation, the positively charged nitrogen of piperazine ring placed in the vicinity of negative area of carboxylic side chain of Asp72 (in the PAS) residue forming an electrostatic bond. The aromatic pyrano coumarin moiety oriented towards the AChE *via* T-shaped π-π interaction with Trp279 residue in the PAS of AChE. Finally, a hydrogen bond between amide nitrogen of **6c** and hydroxyl group of Tyr121 (in the PAS) led to more stabilized interaction.

It is worthwhile mentioning that the obtained results were in good agreement with those obtained in kinetic study.

3. Conclusion

Considering the fact cholinesterase inhibitors have shown the best evidence to alleviating the AD symptoms to date, as they play a key role in cholinergic signaling. In this respect, AChEI's and BuChEI's may pronounce diversity in beneficial effects as far as the severity of the disorder is concerned. Also, selective AChE inhibitors can slow down the amylodgenic product formation (non-catalytic function of AChE) besides increasing the levels of ACh.

In this work, a novel series of pyrano [3,2-*c*]chromen bearing morpholine/phenylpiperazine were synthesized and evaluated against AChE/BuChE using modified Ellman's method. Results showed that among the sixteen synthesized compounds, five exhibited good, selective AChE inhibitory activity. Compound **6c** bearing a phenylpiperazine moiety and 4-methoxypheny moieties showed the highest inhibitory activity (IC_{50} = 1.12 μM) with significant selectivity towards AChE (SI = 40.8) and good neuroprotective activity against H_2O_2 induced oxidative stress. Also, docking study of compound **6c** confirmed those valuable interactions with both the PAS and CAS of AChE. The results of the current research shows that pyrano[3,2-*c*] chromone skeleton may be a new probe for development new agents with potential anti Alzheimer activity.

4. Experimental

4.1. General

All commercially available materials and reagents were purchased from Merck and Aldrich with no further purification. Thin layer chromatography was performed using silica gel 250 μm and F254 plates. Melting points were obtained using Koftler hot stage apparatus. The IR spectra were recorded on Nicolet FT magna 550 spectrograph (KBr pellets). ^{1}H and ^{13}C NMR spectra were recorded on Bruker 500 Hz and the chemical shifts, coupling constants (*J*) are expressed in parts per millennium (ppm) and hertz (Hz), respectively. Mass spectra were acquired on an Agilent Technology (HP) mass spectrometer operating at an ionization potential of 70 eV.

4.2. General procedure for the synthesis of **6a–h** and **7a–h**

A mixture of 4-hydroxycoumarin (**1**) (10 mmol), malanonitrile (**2**) (10 mmol), different aromatic aldehydes (10 mmol) **3**, and DABCO (9 mmol) in EtOH (25 mL) was stirred overnight at room temperature. The precipitate formed was filtered off and washed with EtOH to furnish the pure compound **4** (85–95%). In the next step, Chloroacetyl chloride (12 mmol) was added to the solution of compound **4** (6 mmol) in DMF (30 mL) at 0 °C. Then, the reaction was left to stir at room temperature for 24 h. Reaction progress was monitored by TLC and after completion of the reaction, the mixture was poured into ice cold water and the precipitate was filtered off, dried, and purified by washing with CH_2Cl_2 to afford compounds **5** (35–60%). However, they could be recrystallized from MeOH. Finally, the desired compounds were prepared by reacting intermediate **5** (2 mmol) with phenylpiperazine/morpholine (4 mmol) in methanol in presence of KI under reflux for 18–20 h. The reaction progress was monitored by TLC and the precipitate formed was filtered off and washed with MeOH to remove KI. Finally, the crude products were purified by plate chromatography to afford the desired product in good to high yields (70–85%).

4.2.1. N-(3-Cyano-5-oxo-4-phenyl-4,5-dihydropyrano[3,2-c] chromen-2-yl)-2-(4-phenylpiperazin-1-yl)acetamide (**6a**)

White solid; yield 77%; mp = 243–245 °C; IR (KBr): 3379, 2192, 1711, 1675, 1605 cm^{-1}. ^{1}H NMR (500 MHz, $CDCl_3$): 8.01 (d, *J* = 8.0 Hz, 1H, H5), 7.73 (t, *J* = 8.0 Hz, 1H, H7), 7.52–7.47 (m, H6, H8), 7.33 (d, *J* = 7.0 Hz, 2H, H2′, H6′), 7.26 (t, *J* = 7.0 Hz, 2H, H3′ H5′), 7.22–7.17 (m, 3H, H4′, phenylpiperazine), 6.92 (d, *J* = 7.5 Hz, 2H, phenylpiperazine), 6.77 (t, *J* = 7.5 Hz, 1H, phenylpiperazine), 4.90 (s, 1H, CH), 3.47 (s, 2H, CH_2), 3.15 (t, *J* = 4.0 Hz, 4H, 2×CH_2), 2.66–2.64 (m, 4H, 2×CH_2). ^{13}C NMR (125 MHz, $CDCl_3$): 160.7, 159.8, 159.7, 157.6, 154.2, 152.2, 141.1, 132.0, 128.7, 128.2, 127.9, 126.9, 123.9, 123.5, 122.4, 120.0, 116.3, 116.0, 113.0, 105.3, 103.4, 59.1, 52.8, 48.7, 34.4. Anal. Calcd for $C_{31}H_{26}N_4O_4$: C, 71.80; H, 5.05; N, 10.80. Found: C, 71.49; H, 5.47; N, 10.55.

4.2.2. N-(3-Cyano-4-(2,4-dimethylphenyl)-5-oxo-4,5-dihydropyrano [3,2-c]chromen-2-yl)-2-(4-phenylpiperazin-1-yl)acetamide (**6b**)

White solid; yield 80%; mp >250 °C; IR (KBr): 3283, 2214, 1729, 1676, 1628 cm^{-1}. ^{1}H NMR (500 MHz, DMSO-d_6): 7.97 (d, *J* = 7.5 Hz, 1H, H5), 7.69 (t, *J* = 7.5 Hz, 1H, H7), 7.48–7.42 (m, 2H, H6, H8), 7.19 (t, *J* = 7.0 Hz, 2H, phenylpiperazine), 6.91–6.82 (m, 5H, H3′, H5′, H6′, phenylpiperazine), 6.76 (t, *J* = 7.0 Hz, 1H, phenylpiperazine), 5.01 (s, 1H, CH), 3.49 (s, 2H, CH_2), 3.15–3.13 (m, 4H, 2×CH_2), 2.69–2.65 (m, 7H, 2×CH_2, CH_3), 2.15 (s, 3H, CH_3). ^{13}C NMR (125 MHz, DMSO-d_6): 161.7, 159.8, 158.9, 158.5, 154.0, 151.8, 150.9, 138.8, 136.8, 135.6, 132.7, 130.2, 128.8, 128.3, 126.8, 124.8, 122.6, 118.8, 116.4, 115.4, 113.2, 106.3, 103.6, 59.6, 52.5, 48.1, 29.9, 20.4, 19.3. Anal. Calcd for $C_{33}H_{30}N_4O_4$: C, 72.51; H, 5.53; N, 10.25. Found: C, 72.34; H, 5.47; N, 10.40.

4.2.3. N-(3-Cyano-4-(4-methoxyphenyl)-5-oxo-4,5-dihydropyrano [3,2-c]chromen-2-yl)-2-(4-phenylpiperazin-1-yl)acetamide (**6c**)

White solid; yield 85%; mp >250 °C; IR (KBr): 3419, 2194, 1734, 1666 cm^{-1}. ^{1}H NMR (500 MHz, DMSO-d_6): 7.99 (d, *J* = 8.0 Hz, 1H, H5), 7.72 (td, *J* = 8.0, 1.5 Hz, 1H, H7), 7.50–7.46 (m, 2H, H6, H8), 7.23–7.18 (m, 4H, phenylpiperazine), 6.91 (d, *J* = 8.5 Hz, 2H, H3′, H5′), 6.81 (d, *J* = 8.5 Hz, 2H, H2′, H6′), 6.76 (t, *J* = 7.0 Hz, 1H, phenylpiperazine), 4.83 (s, 1H, CH), 3.68 (s, 3H, OCH_3), 3.44 (s, 2H, CH_2), 3.15 (m, 4H, 2×CH_2), 2.62 (m, 4H, 2×CH_2). ^{13}C NMR (125 MHz, DMSO-d_6): 161.7, 159.8, 159.0, 158.8, 158.2, 154.2, 152.0, 150.9, 134.4, 132.8, 129.6, 128.9, 124.9, 122.7, 118.9, 116.6, 115.4, 113.5, 113.3, 105.3, 102.7, 59.7, 55.0, 52.5, 48.1, 33.6. Anal. Calcd for $C_{32}H_{28}N_4O_5$: C, 70.06; H, 5.14; N, 10.21. Found: C, 69.84; H, 5.37; N, 10.40.

4.2.4. N-(3-Cyano-4-(2,4-dimethoxyphenyl)-5-oxo-4,5-dihydropyrano[3,2-c]chromen-2-yl)-2-(4- phenylpiperazin-1-yl) acetamide (**6d**)

White crystals; yield 70%; mp >250 °C; IR (KBr): 3281, 2219, 1731, 1681 cm^{-1}. ^{1}H NMR (500 MHz, $CDCl_3$): 8.08 (d, *J* = 7.5 Hz, 1H, H5), 7.58 (td, *J* = 7.5, 1.0 Hz, 1H, H7), 7.52 (d, *J* = 8.5, 1H, H6′), 7.38–7.34 (m, 2H, H6, H8), 7.28–7.26 (t, *J* = 7.9 Hz, 2H, phenylpiperazine), 6.94–6.90 (m, 4H, phenylpiperazine, H3′), 6.48 (dd, *J* = 8.5, 2.2 Hz 1H, 5′), 5.15 (s, 1H, CH), 3.74 (s, 3H, OCH_3), 3.65 (s, 2H, CH_2), 3.61 (s, 3H, OCH_3), 3.27–3.25 (m, 4H, 2×CH_2), 2.82–2.80 (m, 4H, 2×CH_2). ^{13}C NMR (125 MHz, $CDCl_3$): 161.5, 160.8, 160.6, 160.5, 159.1, 157.4, 155.1, 152.7, 133.0, 132.0, 129.2, 124.2, 122.6, 120.7, 120.4, 120.3, 116.7, 116.4, 113.8, 104.2, 104.1, 102.4, 99.3, 59.7, 55.3, 55.2, 53.2, 49.2, 32.5. Anal. Calcd for $C_{33}H_{30}N_4O_6$: C, 68.50; H, 5.23; N, 9.68. Found: C, 68.44; H, 5.36; N, 9.40.

4.2.5. N-(3-Cyano-4-(3,4-dimethoxyphenyl)-5-oxo-4,5-dihydropyrano[3,2-c]chromen-2-yl)-2-(4-phenylpiperazin-1-yl) acetamide (**6e**)

Yellow crystals; yield 70%; mp = 225–227 °C; IR (KBr): 3325, 3404, 2196, 1710, 1670 cm^{-1}. ^{1}H NMR (500 MHz, $CDCl_3$): 8.05 (d, *J* = 8.0 Hz, 1H, H5), 7.59 (t, *J* = 8.0 Hz, 1H, H7), 7.38–7.33 (m, 2H, H6, H8), 7.26 (t, *J* = 7.5 Hz, 2H, phenylpiperazine), 7.11 (s, 1H, H2′), 6.92–6.62 (m, 4H, phenylpiperazine, H5′), 6.75 (d, *J* = 8.5 Hz, 1H, H6′), 5.15 (s, 1H,CH), 3.87 (s, 3H, OCH_3), 3.86 (s, 3H, OCH_3), 3.62 (s, 2H, CH_2), 3.23 (t, *J* = 4.0 Hz, 4H, 2×CH_2), 2.77 (t, *J* = 4.0 Hz, 4H, 2×CH_2). ^{13}C NMR (125 MHz, $CDCl_3$): 161.3, 160.4, 160.2, 158.4, 154.5, 152.7, 150.7, 148.8, 148.5, 134.5, 132.4, 129.2, 124.4, 122.8, 120.4, 120.3, 116.8, 116.4, 113.6, 113.0, 111.2, 105.9, 103.8, 59.8, 56.0, 55.9, 53.4, 49.2, 34.3. Anal. Calcd for $C_{33}H_{32}N_4O_6$: C, 68.26; H, 5.56; N, 9.65. Found: C, 68.34; H, 5.45; N, 9.92.

4.2.6. N-(3-Cyano-4-(4-flourophenyl)-5-oxo-4,5-dihydropyrano[3,2-c]chromen-2-yl)-2-(4-phenylpiperazine-1-yl)acetamide (**6f**)

Yellow solid; yield 70%; mp = 238–240 °C; IR (KBr): 3427, 2195, 1727, 1668 cm^{-1}. ^{1}H NMR (500 MHz, $CDCl_3$): 8.05 (d, *J* = 7.5 Hz, 1H, H5), 7.58 (t, *J* = 7.5 Hz, 1H, H7), 7.39–7.31 (m, 4H, H6, H8, phenylpiperazine), 7.25 (t, *J* = 7.5 Hz, 2H, H3′, H5′), 6.94–6.83 (m, 4H, H2′, H6′, phenylpiperazine), 6.83 (d, *J* = 7.2 Hz, 1H, phenylpiperazine), 5.14 (s, 1H, CH), 3.62 (s, 2H, CH_2), 3.22 (t, *J* = 4.5 Hz, 4H, 2×CH_2), 2.76 (t, *J* = 4.5 Hz, 4H, 2×CH_2). ^{13}C NMR (125 MHz, $CDCl_3$): 161.9 (d, $J_{C\text{-}F}$ = 245.0 Hz), 161.6, 160.2, 158.8, 154.6, 152.7, 150.7, 137.4, 132.5, 130.3, 130.2, 129.1, 124.4, 122.8, 120.1, 116.7, 116.2, 115.1 (d, $J_{C\text{-}F}$ = 25.0 Hz), 113.4, 105.5, 103.3, 59.8, 53.3, 49.0, 34.2. MS (*m*/*z*, %): 536 (M^+, 9), 376 (13), 280 (40), 161 (29), 132 (100), 104 (40), 77 (27), 56 (36). Anal. Calcd

for $C_{31}H_{25}FN_4O_4$: C, 69.39; H, 4.70; N, 10.44. Found: C, 69.60; H, 4.44; N, 10.30.

4.2.7. N-(4-(4-Chlorophenyl)-3-cyano-5-oxo-4,5-dihydropyrano[3,2-c]chromen-2-yl)-2-(4-phenylpiperazin-1-yl)acetamide (**6g**)

White crystals; yield 70%; mp >250 °C; IR (KBr): 3467, 2225, 1729, 1678 cm^{-1}. ^1H NMR (500 MHz, $CDCl_3$): 8.01 (d, J = 7.6 Hz, 1H, H5), 7.74 (t, J = 7.5 Hz, 1H, H7), 7.52–7.44 (m, 2H, H6, H8), 7.37 (d, J = 8.3 Hz, 2H, H3′, H5′), 7.32 (d, J = 8.3 Hz, 2H, H2′, H6′), 7.20 (t, J = 7.8 Hz, 2H, phenylpiperazine), 6.92 (d, J = 7.8 Hz, 2H, phenylpiperazine), 6.77 (t, J = 7.8 Hz, 1H phenylpiperazine), 4.8 (s, 1H, CH), 3.68 (s, 2H, CH_2), 3.27 (s, 4H, 2×CH_2), 2.84 (s, 4H, 4H, 2×CH_2). ^{13}C NMR: 161.1, 160.3, 160.2, 158.4, 154.8, 152.8, 150.5, 140.1, 133.3, 132.7, 130.1, 129.3, 128.5, 124.5, 122.9, 120.5, 116.9, 116.5, 113.4, 105.3, 103.4, 59.6, 53.3, 49.1, 34.5 MS (m/z, %): 554 ([M + 2]$^+$, 0.3), 552 (M$^+$, 1), 125 (100), 366 (7), 338 (99), 235 (13), 207 (11), 143 (21), 178 (62), 161 (12), 221 (62), 113 (5), 77 (21). Anal. Calcd for $C_{31}H_{25}ClN_4O_4$: C, 67.33; H, 4.56; N, 10.13. Found: C, 67.20; H, 4.82; N, 9.82.

4.2.8. N-(3-Cyano-4-(4-nitrophenyl)-5-oxo-4,5-dihydropyrano[3,2-c]chromen-2-yl)-2-(4-phenylpiperazin-1-yl)acetamide (**6h**)

Yellow crystals; Yield 77%; mp >250 °C; IR (KBr): 3427, 3266, 2222, 1720, 1681 cm^{-1}. ^1H NMR (500 MHz, DMSO-d_6): 8.12 (d, J = 8.5 Hz, 2H, H3′, H5′), 8.00 (d, J = 7.7 Hz, 1H, H5), 7.75 (t, J = 7.7 Hz, 1H, H7), 7.66 (d, J = 8.5 Hz, 2H, H2′, H6′), 7.53–7.48 (m, 2H, H6, H8), 7.20 (t, J = 7.7 Hz, 2H, phenylpiperazine), 6.91 (d, J = 7.7 Hz, 2H, phenylpiperazine), 6.77 (t, J = 7.7 Hz, 1H, phenylpiperazine), 5.03 (s, 1H, CH), 3.52 (d, J = 14.0 Hz, 1H, CH_2), 3.49 (d, J = 14.0 Hz, 1H, CH_2), 3.18–3.05 (m. 4H, 2×CH_2), 2.74–2.61 (m, 4H, 2×CH_2). ^{13}C NMR (125 MHz, DMSO-d_6): 161.7, 159.8, 159.6, 159.2, 154.9, 152.1, 150.9, 149.6, 146.4, 133.1, 130.2, 128.9, 124.9, 123.1, 122.8, 118.8, 116.6, 115.4, 113.1, 103.9, 101.3, 59.7, 52.5, 48.1, 35.0. MS (m/z, %): 564 (M$^+$, 3), 93 (100), 120 (95), 162 (81), 281 (84), 218 (20). Anal. Calcd for $C_{31}H_{25}N_5O_6$: C, 66.07; H, 4.47; N, 12.43. Found: C, 65.80; H, 4.61; N, 12.64.

4.2.9. N-(3-Cyano-5-oxo-4-phenyl-4,5-dihydropyrano[3,2-c]chromen-2-yl)-morpholinoacetamide (**7a**)

Pale yellow solid; yield 80%; mp >250 °C; IR (KBr): 3379, 2192, 1711, 1675 cm^{-1}. ^1H NMR (500 MHz, DMSO-d_6): 8.01 (d, J = 7.7 Hz, 1H, H5), 7.73 (t, J = 7.7 Hz, 1H, H7), 7.52–7.47 (m, 2H, H6, H8), 7.32 (d, J = 7.2 Hz, 2H, H2′, H6′), 7.26 (t, J = 7.2 Hz, 2H, H3′, H5′), 7.18 (t, J = 7.2 Hz, 1H, H4′), 4.88 (s, 1H, CH), 3.59–3.57 (m, 6H, 3×CH_2), 3.40–3.38 (m, 4H, 2×CH_2). ^{13}C NMR (125 MHz, DMSO-d_6): 154.7, 153.1, 142.5, 139.2, 138.6, 137.6, 132.9, 128.6, 128.2, 126.9, 125.1 124.9, 124.4, 122.7, 118.2, 116.6, 113.4, 66.1, 60.3, 53.1, 34.5. Anal. Calcd for $C_{25}H_{21}N_3O_5$: C, 67.71; H, 4.77; N, 9.48. Found: C, 67.64; H, 4.50; N, 9.74.

4.2.10. N-(3-Cyano-4-(4-methoxyphenyl)-5-oxo-4,5-dihydropyrano[3,2-c]chromen-2-yl)-2-morpholineacetamide (**7b**)

White solid; yield 80%; mp = 242–245 °C; IR (KBr): 3417, 2204, 1734, 1665 $cm^{-1}cm^{-1}$. ^1H NMR (500 MHz, DMSO-d_6) : 7.97 (dd, J = 7.7, 1.5 Hz, 1H, H5), 7.72 (td, J = 7.7, 1.5 Hz, 1H, H7), 7.50–7.46 (m, 2H, H6, H8), 7.21 (d, J = 6.5 Hz, 2H, H2′, H6′), 6.80 (d, J = 7.5 Hz, 2H, H3′, H5′), 4.82 (s, 1H, CH), 3.68 (s, 3H, OCH_3), 3.57 (s, 2H, CH_2), 3.45–3.41 (m, 8H, 4×CH_2). ^{13}C NMR (125 MHz, DMSO-d_6): 161.8, 159.9, 159.1, 158.8, 158.2, 154.3, 152.1, 134.5, 133.0, 129.6, 124.9, 122.7, 116.6, 113.6, 113.3, 105.3, 102.7, 66.1, 60.1, 55.1, 53.1, 33.6. Anal. Calcd for $C_{26}H_{23}N_3O_6$: C, 65.95; H, 4.90; N, 8.87. Found: C, 65.69; H, 4.67; N, 8.74.

4.2.11. N-(3-Cyano-4-(2,4-dimethoxyphenyl)-5-oxo-4,5-dihydropyrano[3,2-c]chromen-2-yl)-2-morpholinoacetamide (**7c**)

Yellow crystals; yield 75%; mp >250 °C; IR (KBr): 3281, 3001, 2968, 2944, 2219, 1735, 1681, 1611 cm^{-1}. ^1H NMR (500 MHz, DMSO-d_6): 8.01 (d, J = 7.5 Hz, 1H, H5), 7.69 (t, J = 7.5 Hz, 1H, H7), 7.49–7.43 (m, 2H, H6, H8), 7.25 (d, J = 8.5 Hz, 1H, H6′, 1H), 6.46 (dd, J = 8.5, 1.5 Hz, 1H, H5′), 6.41 (s, 1H, H3′), 4.83 (s, 1H,CH), 3.69–3.52 (m, 16 H, 5×CH_2, 2×OCH3). ^{13}C NMR (125 MHz, DMSO-d_6): 160.1, 159.7, 158.9, 155.0, 152.0, 151.1, 132.7, 132.5, 124.8, 132.5, 122.5, 121.7, 121.6, 116.5, 113.6, 104.6, 103.8, 103.6, 99.1, 66.1, 61.3, 55.7, 55.1, 53.1, 32.0. Anal. Calcd for $C_{27}H_{25}N_3O_6$: C, 64.41; H, 5.00; N, 8.35. Found: C, 64.61; H, 4.87; N, 8.54.

4.2.12. N-(3-Cyano-4-(3,4-dimethoxyphenyl)-5-oxo-4,5-dihydropyrano[3,2-c]chromen-2-yl)-2-morpholinoacetamide (**7d**)

Yellow crystals; yield 75%; mp = 235–237 °C; IR (KBr): 3385, 3005, 2978, 2205, 1717, 1665 cm^{-1}. ^1H NMR (500 MHz, $CDCl_3$): 8.04 (d, J = 7.0 Hz, 1H, H5), 7.58 (td, J = 7.0, 1.0 Hz, 1H, H7), 7.38–7.34 (m, 2H, H6, H8), 7.12 (d, J = 1.5 Hz, 1H, H2′), 6.83–6.80 (dd, J = 7.7, 1.5 Hz, 1H, H5′), 6.75 (d, J = 7.7 Hz, 1H, H6′), 5.14 (s, 1H, CH), 3.87 (s, 3H, OCH_3), 3.79 (s, 3H, OCH_3), 3.75–3.73 (t, J = 4.5 Hz, 4H, 2×CH_2), 3.56 (d, J = 15.0 Hz, 1H, CH_2), 3.54 (d, J = 15.0 Hz, 1H, CH_2), 2.61–2.59 (t, J = 4.5 Hz, 4H, 2×CH_2). ^{13}C NMR (125 MHz, $CDCl_3$): 161.7, 160.4, 160.3, 158.4, 154.4, 152.6, 148.7, 148.4, 134.4, 132.4, 124.3, 122.8, 120.4, 116.7, 113.5, 112.8, 111.1, 105.8, 103.5, 66.5, 60.3, 56.0, 55.8, 53.8, 53.5, 53.3, 34.2. Anal. Calcd for $C_{27}H_{25}N_3O_6$: C, 64.41; H, 5.00; N, 8.35. Found: C, 64.40; H, 5.17; N, 8.39.

4.2.13. N-(3-Cyano-4-(4-flourophenyl)-5-oxo-4,5-dihydropyrano[3,2-c]chromen-2-yl)-2-morpholinoacetamide (**7e**)

White solid; yield 70%; mp >255 °C; IR (KBr): 3421, 3018, 2978, 2185, 1717, 1667 cm^{-1}. ^1H NMR (500 MHz, DMSO-d_6): 8.55 (s, 1H, NH), 7.99 (d, J = 7.7 Hz, 1H, H5), 7.71 (t, J = 7.7 Hz, 1H, H7), 7.50–7.45 (m, 2H, H6, H8), 7.34 (dd, J = 8.0, 5.5 Hz, 2H, H2′, H6′), 7.15 (t, J = 8.0 Hz, 2H, H3′, H5′), 4.58 (s, 1H, CH), 3.40–3.38 (m, 4H, 2×CH_2), 3.25 (s, 2H, CH_2), 3.04–3.02 (m, 4H, 2×CH_2). ^{13}C NMR (125 MHz, DMSO-d_6): 161.0 (d, $J_{C\text{-}F}$ = 240.0 Hz), 160.6, 159.5, 154.9, 152.1, 146.8, 146.6, 139.2, 132.8, 130.4 (d, $J_{C\text{-}F}$ = 8.7 Hz), 124.8, 122.8, 116.6, 114.7 (d, $J_{C\text{-}F}$ = 21.2 Hz), 113.5, 105.2, 100.7, 66.1, 61.6, 53.2, 34.0. Anal. Calcd for $C_{25}H_{20}FN_3O_5$: C, 65.07; H, 4.37; N, 9.11 Found: C, 65.41; H, 4.17; N, 9.37.

4.2.14. N-(4-(4-Chlorophenyl)-3-cyano-5-oxo-4,5-dihydropyrano[3,2-c]chromen-2-yl)-2-morpholinoacetamide (**7f**)

White crystals; yield 70%; mp >250 °C; IR (KBr): 3467, 3272, 2225, 1729, 1678, cm^{-1}. ^1H NMR (500 MHz, $CDCl_3$): 8.05 (dd, J = 8.0, 1.5 Hz, 1H, H5), 7.60 (td, J = 7.7, 1.5 Hz, 1H, H7), 7.39–7.34 (m, 4H, H6, H8, H3′, H5′), 7.23 (d, J = 9.0 Hz, 2H, H2′, H6′), 5.15 (s, 1H, CH), 3.74 (t, J = 4.5 Hz, 4H, 2×CH_2), 3.56 (d, 2H, J = 14.0 Hz, 1H, CH_2), 3.53 (d, 2H, J = 14.0 Hz, 1H, CH_2), 2.60 (t, 4H, J = 4.5 Hz, 4H, 2×CH_2). ^{13}C NMR (125 MHz, $CDCl_3$): 160.9, 160.3, 158.6, 154.8, 152.8, 140.2, 133.3, 132.6, 130.1, 128.5, 126.0, 124.5, 122.9, 116.9, 113.5, 105.4, 103.4, 66.6, 60.3, 53.7, 34.5. MS (m/z, %): 479 ([M+2]$^+$, 2), 477 (M$^+$, 6), 86 (100), 392 (44), 281 (86), 240 (55), 121 (32). Anal. Calcd for $C_{25}H_{20}ClN_3O_5$: C, 62.83; H, 4.22; N, 8.79. Found: C, 62.64; H, 4.40; N, 8.44.

4.2.15. N-(3-Cyano-4-(4-nitrophenyl)-5-oxo-4,5-dihydropyrano[3,2-c]chromen-2-yl)-2-morpholinoacetamide (**7g**)

White crystals; yield 70%; mp = 216–218 °C, white crystals; IR (KBr): 3265, 2223, 1703, 1682 cm^{-1}. ^1H NMR (500 MHz, $CDCl_3$): 10.20 (bs, 1H, NH), 8.14–8.05 (m, 3H, H5, H3′, H5′), 7.61–7.59 (m, 3H, H7, H2′, H6′), 7.40–7.35 (m, 2H, H6, H8), 5.27 (s, 1H,CH), 3.74–3.73 (m, 4H, 2×CH_2), 3.60 (s, 2H, CH_2), 2.60–2.59 (m, 4H,

2×CH_2).^{13}C NMR (125 MHz, $CDCl_3$): 160.7, 160.5, 160.1, 159.2, 155.3, 152.9, 148.6, 147.3, 133.1, 129.8, 124.7, 123.7, 123.1, 117.0, 113.3, 104.5, 102.6, 66.6, 60.2, 53.7, 35.2. Anal. Calcd for $C_{25}H_{20}N_4O_7$: C, 61.48; H, 4.13; N, 11.47. Found: C, 61.65; H, 4.28; N, 11.47.

*4.2.16. N-(3-Cyano-5-oxo-4-(thiophene-2-yl)-4,5-dihydropyrano[3,2-c]chromen-2-yl)-2-morpholinoacetamide (**7h**)*

Light pink crystals; yield 70%; mp >250 °C; IR (KBr): 3233, 3192, 2221, 1717, 1677 cm^{-1}. ^{1}H NMR (500 MHz, DMSO-d_6): 7.97 (d, J = 8.0 Hz, 1H, H5), 7.75 (t, J = 8.0 Hz, 1H, H7), 7.51–7.47 (m, 2H, H6, H8), 7.34 (d, J = 4.5 Hz, 1H, thiophene), 6.98 (d, J = 4.5 Hz, 1H, thiophene), 6.92 (t, J = 4.5 Hz, 1H, thiophene), 5.22 (s, 1H, CH), 3.61 (t, J = 4.3 Hz, 4H, 2×CH_2), 3.46–3.44 (m, 6H, 3×CH_2). ^{13}C NMR (125 MHz, DMSO-d_6): 161.7, 159.8, 159.2, 159.1, 154.5, 152.1, 145.5, 133.1, 126.9, 125.7, 125.5, 125.0, 122.7, 116.7, 113.1, 104.7, 102.0, 66.0, 60.1, 53.0, 29.1. MS (m/z, %): 449 (M^+, 20), 86 (100), 364 (89), 280 (59), 240 (63), 121 (35). Anal. Calcd for $C_{23}H_{19}N_3O_5S$: C, 61.46; H, 4.26; N, 9.35. Found: C, 61.32; H, 4.42; N, 9.52.

4.3. In vitro AChE and BuChE inhibition assays

To evaluation of the biological activity, all synthesized compounds **6** and **7** were subjected to AChE/BuChE inhibition assays using Ellman's method.[23,24] The tested compounds were dissolved in a mixture of 1 mL DMSO and 9 mL ethanol and then four different concentrations of each compound were tested to obtain the range of 20% to 80% enzyme inhibition for AChE and BuChE. For this purpose, in a 24 well plate, 2 mL phosphate buffer (0.1 M, pH = 8.0), 65 μL of DTNB 0.1 M, 35 μL of enzyme [2 U/mL of AChE (E.C. 3.1.1.7, Type V-S, lyophilized powder, from *electric eel*) or BuChE (E.C. 3.1.1.8, from equine serum)] and 35 μL of inhibitor solution or DMSO:EtOH mixture (1:9) was added. Then, 10 μL of substrate 0.15 M (acetylthiocholine iodide or butyrylthiocholine iodide) was added to each well and the change of absorbance was measured at 412 nm for 6 min. The IC_{50} values were determined graphically from inhibition curves (log inhibitor concentration vs. percent of inhibition). All experiments were performed on a synergy HTX microplate reader (kinetic mode) in quadruplicates.

4.4. Kinetic study

To study the kinetic mode of mechanism of compound **6c,** reciprocal plots of 1/velocity *vs.* 1/[S] (substrate) were drawn at three concentrations of substrate acetylthiocholine employing Ellman's method (0.62, 1.23 and 2.47 μM). Initial velocity in each case, was achieved at different concentration of substrate (acetylthiocholine) and for each experiment after adding acetylthiocholine, progress curves were monitored at 420 nm for 2 min. The reciprocal of the velocity was plotted against the reciprocal of substrate.

4.5. Neuroprotection study

PC12 cell line was obtained from Pasteur institute (Tehran, IRAN) and all culture media as well as supplements were purchased from Gibco. Cells were cultivated in DMEM supplemented with 10% fetal calf serum, 5% horse serum and antibiotics (100 units/mL penicillin, 100 μg/mL streptomycin). To induce neuronal differentiation, PC12 cells were re-suspended using trypsin/EDTA (0.25%) and seeded in 96 well culture plate (3000 cells/well) and cultured for 1 week in differentiation medium (DMEM + 2% horse serum + NGF (100 ng/mL) + penicillin & streptomycin). To evaluate the effect of compounds **6c**, **6e**, **6g**, **7b**, and **7d** on survival rate of neurons, the culture medium was changed to NGF free medium and different concentrations of the above mentioned compounds (10, 50, 100 μM) were applied on cells. Quercetin (50 μM) was used as a positive control. Compounds were diluted into DMEM and added 10 μL to each well. Three hours later induction of ROS mediated apoptosis was initiated by adding the H_2O_2 (400 μM) to their medium and after 12 h, MTT assay was performed. MTT solution (5 mg/mL) was added to each well in a volume of 10 μL, and 3 h later culture medium replaced with 100 μL of DMSO. Absorbance at 545 nm was measured using an ELISA reader. Each experimental was performed in four replicates.

4.6. BACE1 enzymatic assay

A FRET-based BACE1 enzyme assay kit was purchased from Invitrogen (former Pan Vera Corporation, Madison, WI) and the assay was carried out according to the manufacturer's instructions (Invitrogen. http://tools.invitrogen.com/content/sfs/manuals/L0724.pdf).[24]

4.7. Statistical analysis

The statistical analysis was carried out by graph pad prism 6. Data is expressed as mean ± SD. One-way analysis of variance (ANOVA) was used to analyze the data in conjugation with tukey's test to determine the data significance by single- step multiple comparisons.

4.8. Docking simulation method

The pdb file of the receptor (1EVE) complexed with E2020 (donepezil) was retrieved from the Brookhaven protein database http://www.rcsb.org/pdb/home/home.do. Subsequently, the co-crystallized ligand, water molecules were removed and polar hydrogen were added using Discovery Studio 4.1. The structures of compound **6c** were sketched and saved in pdb format using Marvin Sketch 15.6.8 www.chemaxon.com. The ligand molecule **6c** was saved in pdbqt format after adding Kollman charges. The pdbqt file of ligands was prepared in Auto Dock tools 1.5.6rc The active site of receptor pdb file for docking was created with dimensions 60, 60, 60 with co-ordinates x, y, z of grid box was set as default. The results were visualized in Discovery Studio 4.1 as 2D and 3D diagrams.

3D structure of AChE in complex with E2020 (Donepezil) with ID number: 1eve was retrieved from Brook-haven Protein data bank (www.rcsb.org). To prepare protein for docking simulation, all co-crystallized and water molecules was removed and the protein was converted to required pdbqt format using Auto dock Tools package (1.5.6).[26] The 2D structure of ligand was prepared using Marvin Sketch 5.8.3, 2012, Chem Axon(www.chemaxon.com); then, 2D structure was converted to 3D format by Openbabel (ver 2.3.1)[27] and finally, pdbqt format of ligand was prepared using Auto dock Tools python script, *prepare_ligand4.py*

Docking simulations were performed with Autodock Vina[28] (1.1.2) within a docking box defined by following parameters: size_x = 15, size_y = 15, size_z = 15 Å, center_x = 2.023, center_y = 63.295, center_z = 67.062. The exhaustiveness was set to 80 and the other docking parameters were set as default. At the end of docking simulations, the best docking solutions were selected for further analysis of enzyme-inhibitor interactions. The graphics are depicted using chimera 1.10.2 and Biovia discovery studio visualizer.[29]

Acknowledgements

This work was financially supported by Research Council of Tehran University of Medical Sciences, International Campus

(TUMS-IC) vide grant No. 93-01-103-25020. Late Prof. Abbas Shafiee is highly acknowledged for providing me insight and all over support in this work.

References

1. Walsh DM, Selkoe DJ. Deciphering the molecular basis of memory failure in Alzheimer's disease. *Neuron*. 2004;44:181–193.
2. Francis PT, Palmer AM, Snape M, Wilcock GK. The cholinergic hypothesis of Alzheimer's disease: a review of progress. *J Neurol Neurosurg Psychiatry J Neurol Neurosurg Psychiatry*. 1999;66:137–147.
3. LaFerla FM, Green KN, Oddo S. Intracellular amyloid-beta in Alzheimer's disease. *Nat Rev Neurosci*. 2007;8:499–509.
4. Oakley H, Cole SL, Logan S, et al. Intraneuronal beta-amyloid aggregates, neurodegeneration, and neuron loss in transgenic mice with five familial Alzheimer's disease mutations: potential factors in amyloid plaque formation. *J Neurosci*. 2006;26:10129–10140.
5. Smith MA, Zhu X, Tabaton M, et al. Increased iron and free radical generation in preclinical Alzheimer disease and mild cognitive impairment. *Alzheimers Dis*. 2010;19:363–372.
6. Alvarez A, Bronfman F, Perez CA, Vicente M, Garrido J, Inestrosa NC. Acetylcholinesterase, a senile plaque component, affects the fibrillogenesis of amyloid-beta-peptides. *Neurosci Lett Neurosci Lett*. 1995;201:49–52.
7. Jacobsen JS, Reinhart P, Pangalos MN. Current concepts in therapeutic strategies targeting cognitive decline and disease modification in Alzheimer's disease. *NeuroRx*. 2005;2:612–626.
8. Darvesh S, Hopkins DA, Geula C. Neurobiology of butyrylcholinesterase. *Nat Rev Neurosci*. 2003;4:131–138.
9. Greig NH, Lahiri DK, Sambamurti K. Butyrylcholinesterase: an important new target in Alzheimer's disease therapy. *Int Psychogeriatr*. 2002;14:77–91.
10. Marumoto S, Miyazawa M. Structure–activity relationships for naturally occurring coumarins as β-secretase inhibitor. *Bioorg Med Chem*. 2012;20:784–788.
11. Cai Z, Zhao B, Ratka A. Oxidative stress and β-amyloid protein in Alzheimer's disease. *Neuromol Med*. 2011;13:250.
12. Mehta M, Adem A, Sabbagh M. New Acetylcholinesterase Inhibitors for Alzheimer's disease. *Int J Alzheimers Dis*. 2012;2012:1–8.
13. McGleenon BM, Dynan KB, Passmore AP. Acetylcholinesterase inhibitors in Alzheimer's disease. *J Clin Pharmacol*. 1999;48:471–480.
14. Anand P, Singh B, Singh N. A review on coumarins as acetylcholinesterase inhibitors for Alzheimer's disease. *Bioorg Med Chem*. 2012;20:1175–1180.
15. Piazzi L, Rampa A, Bisi A, et al. 3-(4-[[Benzyl(methyl)amino]methyl]phenyl)-6,7-dimethoxy-2H-2-chromenone (AP2238) inhibits both acetylcholinesterase and acetylcholinesterase-induced beta-amyloid aggregation: a dual function lead for Alzheimer's disease therapy. *J Med Chem*. 2003;46:2279–2282.
16. Hilgert M, Nöldner M, Chatterjee SS, Klein J. KA-672 inhibits rat brain acetylcholinesterase in vitro but not in vivo. *Neurosci Lett*. 1999;263:193–196.
17. Sameem B, Saeedi M, Mahdavi M, Shafiee A. A review on tacrine-based scaffolds as multi-target drugs (MTDLs) for Alzheimer's disease. *Eur J Med Chem*. 2017. in press.
18. Ebrahimi SES, Ghadirian P, Emtiazi H, et al. Hetero-annulated coumarins as new AChE/BuChE inhibitors: synthesis and biological evaluation. *Med Chem Res*. 2016;25:1831–1841.
19. Najafi Z, Mahdavi M, Saeedi M, et al. Novel tacrine-1,2,3-triazole hybrids: In vitro, in vivo biological evaluation and docking study of cholinesterase inhibitors. *Eur J Med Chem*. 2017. In press.
20. Saeedi M, Golipoor M, Mahdavi M, et al. Phthalimide-derived N-benzylpyridinium halides targeting cholinesterases: synthesis and bioactivity of new potential anti-Alzheimer's disease agents. *Arch Pharm*. 2016;349:293–301.
21. Irannejad H, Amini M, Khodagholi F, et al. Synthesis and in vitro evaluation of novel 1,2,4-triazine derivatives as neuroprotective agents. *Bioorg Med Chem*. 2010;18:4224–4230.
22. Khoobi M, Alipour M, Moradi A, et al. Design, synthesis, docking study and biological evaluation of some novel tetrahydrochromeno [3',4':5,6]pyrano[2,3-b]quinolin-6(7H)-one derivatives against acetyl- and butyrylcholinesterase. *Eur J Med Chem*. 2013;68:291–300.
23. Gorun V, Proinov I, Băltescu V, Balaban G, Bârzu O. Modified Ellman procedure for assay of cholinesterases in crude enzymatic preparations. *Anal Biochem*. 1986;86:324–326.
24. Ellman GL, Courtney KD, Andres V, Feather-Stone JRM. A new and rapid colorimetric determination of acetylcholinesterase activity. *Biochem Pharmacol*. 1961;7:88–95.
25. Najafi Z, Saeedi M, Mahdavi M, et al. Design and synthesis of novel anti-Alzheimer's agents: Acridine-chromenone and quinoline-chromenone hybrids. *Bioorg Med Chem*. 2016;67:84–94.
26. Sanner MF. A programming language for software integration and development. *J Mol Graph Model*. 1999;17:57–61.
27. O'Boyle NM, Banck M, James CA, Morley C, Vandermeersch T, Hutchison GR. Design and synthesis of novel anti-Alzheimer's agents: Acridine-chromenone and quinoline-chromenone hybrids. *J Cheminformatics*. 2011;3:33.
28. Trott O, Olson AJ. Improving the speed and accuracy of docking with a new scoring function, efficient optimization, and multithreading. *J Comput Chem*. 2010;31:455–461.
29. Pettersen EF, Goddard TD, Huang CC, et al. UCSF Chimera–a visualization system for exploratory research and analysis. *J Comput Chem*. 2004;25:1605–1612.